Pergamon

Geochimica et Cosmochimica Acta, Vol. 60, No. 12, pp. 2111–2121, 1996

0016-7037/96 $15.00 + .00

PII S0016-7037(96)00091-9

Schwertmannite and the chemical modeling of iron in acid sulfate waters

J. M. BIGHAM,[1] U. SCHWERTMANN,[2] S. J. TRAINA,[1] R. L. WINLAND,[1] and M. WOLF[3]

[1]School of Natural Resources, The Ohio State University, Columbus, OH 43210, USA
[2]Lehrstuhl für Bodenkunde, Technische Universität München, D-85350 Freising-Weihenstephan, Germany
[3]Institut für Hydrologie, GSF-Neuherberg, D-85764 Oberschleißheim, Germany

(*Received March* 2, 1995; *accepted in revised form March* 4, 1996)

Abstract—Analyses of ochreous sediments and associated solutions from twenty-eight mine drainage sites showed that precipitates formed at pH 6.5 or higher were composed of ferrihydrite (nominally $Fe_5HO_8 \cdot 4H_2O$) or a mixture of ferrihydrite and goethite (α-FeOOH), whereas those precipitated from waters having pH values in the range of 2.8 to 4.5 were predominantly schwertmannite (ideally $Fe_8O_8(OH)_6SO_4$) with trace to minor amounts of goethite. Solutions of intermediate pH values produced mixtures of ferrihydrite and schwertmannite. Only one sample, formed at pH 2.6, contained a significant amount of jarosite (H, K, Na)$Fe_3(OH)_6(SO_4)_2$. A solubility window of log IAP_{Sh} = 18.0 ± 2.5 was calculated for schwertmannite from selected mine drainage solutions with pH values in the range of 2.8 to 3.2. The relationship between pH and log $a_{Fe^{3+}}$ over the full range of drainage waters was consistent with published results from other sources, and the combined mineralogy-chemistry data were used to compute a new pe-pH diagram for the system Fe–S–K–O–H that included a field of metastability for schwertmannite. The metastable nature of schwertmannite was confirmed in a long-term (1739 d) aqueous equilibrium study wherein a pure, synthetic specimen was completely transformed to goethite over a period of 543 days. The pH and computed activity of Fe^{3+} in the final equilibrium solutions yielded a log K_{Gt} = 1.40 ± 0.01 for goethite. Additional field data supporting a paragenetic relationship between jarosite, schwertmannite, ferrihydrite, and goethite were obtained from a naturally acid alpine stream. Similar results were predicted from the water chemistry using a nonequilibrium reaction path model that included appropriate solubility data for the mineral phases of interest.

1. INTRODUCTION

Acid sulfate waters (ASW) are produced by the aerobic leaching of sulfide-bearing rocks, sediments, and soils. Usually, ASW are associated with anthropogenic activities such as mining or soil drainage, but strictly natural occurrences also exist (e.g., Theobald et al., 1963; Schwertmann et al., 1995). A variety of chemical models are now being used by geochemists, hydrologists, and engineers as tools for understanding the formation of ASW and the subsequent dispersion of dissolved pollutants in surface and groundwaters. These models are affected by numerous chemical, physical, and biological factors that are not always easily quantified (McKnight and Bencala, 1989). The most common uncertainties arise from problems associated with redox disequilibria, the calculation of charge imbalances, inaccurate measurements of very acid pH values, and inadequate estimates of stability constants (Nordstrom et al., 1990; Nordstrom, 1991).

A general lack of knowledge regarding the mineralogy of sulfide-rich tailings/waste rocks and their oxidation products also represents a serious deficiency in most hydrogeochemical studies of ASW (Jambor, 1994). The absence of site-specific mineralogical information is important because, without it, errors regarding mineral-solution equilibria are almost inevitable. In particular, the identification of solid phases purely on the basis of solution chemistry and equilibrium solubility calculations offers little hope for valid conclusions when the thermodynamic database for relevant minerals is either widely variable or unavailable.

In this regard, a new mineral has recently been identified that may be the dominant solid phase controlling the activities of both major and minor elements in ASW (Bigham et al., 1994). This mineral, schwertmannite, is poorly crystalline with a tunnel structure akin to that of akaganéite (nominally β-FeOOH). Its ideal formula is $Fe_8O_8(OH)_6SO_4$ but may range to $Fe_8O_8(OH)_{4.5}(SO_4)_{1.75}$ depending upon the degree to which tunnel and surface sites are saturated with sulfate. Additional details regarding the properties of schwertmannite are given elsewhere (Bigham et al., 1990; Murad et al., 1994). The objectives of the current paper are to (1) describe the paragenetic relationships that appear to exist between schwertmannite and associated minerals in ochreous precipitates formed from sulfate-rich waters over a wide range of pH, (2) evaluate the stability and aqueous solubility of schwertmannite using both field and laboratory data, and (3) demonstrate the importance of this information for the geochemical modeling of ASW.

2. MATERIALS AND METHODS

2.1. Stability Study

Mineralogically pure samples of schwertmannite were prepared in triplicate using an abiotic synthesis procedure similar to that described by Bigham et al. (1990). Two L of a 0.02 M solution of K_2SO_4 was warmed to 60°C. Sufficient solid $Fe(NO_3)_3 \cdot 9H_2O$ was then added to yield a solution that was also 0.02 M in Fe (hereafter, the use of an elemental or molecular formula without charge notation indicates the total analytical concentration in solution without regard to valence or the possible existence of ion pairs or other complex species). The resulting forced hydrolysis of Fe(III) (hereafter, a Roman numeral will be used to indicate all possible aqueous species of an element having the indicated oxidation state) produced a

Table 1. Mineralogy of precipitates and pH of source waters

Site	Mineralogy†		pH		Fe_O/Fe_{tot}		Fe_{tot}/S_{tot}‡
Jf-1	Gt, Fh		7.3		0.43		480.0
Bt-1	Gt, Fh		6.8		0.43		128.9
		avg.	7.0	avg.	0.43	avg.	304.5
Jf-2	Fh		7.8		0.99		83.8
Bt-3	Fh		7.5		0.91		55.3
Tu-4	Fh		6.8		1.00		37.0
		avg.	7.2	avg.	0.97	avg.	58.7
Ms-2	Fh, Sh		6.1		0.94		8.6
Ms-1	Fh, Sh		5.8		0.91		9.9
Jk-2	Fh, Sh		4.9		0.98		10.6
		avg.	5.3	avg.	0.94	avg.	9.7
Jk-1	Sh, Gt		5.9		0.83		7.2
Pr-3	Sh, Gt		3.3		0.94		5.6
Pr-1	Sh, Gt, Jt(t)		3.2		0.79		5.2
Pr-5	Sh, Gt, Jt(t)		3.1		0.85		4.6
Vn-1	Sh, Gt		3.1		0.77		5.6
Tu-1	Sh, Gt		2.9		0.61		6.2
		avg.	3.2	avg.	0.80	avg.	5.7
Ho-1	Sh, Gt(t)		4.2		0.93		5.9
Tu-2	Sh, Gt(t)		3.2		0.84		5.2
Ms-3	Sh, Gt(t)		2.8		0.91		4.4
La-1	Sh, Gt(t)		3.1		0.94		5.3
Jf-3	Sh		3.8		0.98		6.8
Pr-4	Sh		3.8		0.86		5.6
Me-1	Sh		3.7		0.90		6.5
Pr-2	Sh, Gt(t), Jt(t)		2.8		0.94		6.0
Bt-4	Sh, Gt(t)		3.2		0.99		4.7
Nb-1	Sh, Gt(t), Jt(t)		3.0		0.99		4.9
Cs-1	Sh, Jt(t)		3.3		0.99		5.3
Tu-3	Sh, Jt(t)		3.2		0.95		4.7
Wa-1	Sh, Jt(t)		3.8		0.78		4.4
		avg.	3.2	avg.	0.92	avg.	5.4
Ms-5	Jt, Gt		2.6		0.16		4.4

† Gt = goethite, Fh = ferrihydrite, Sh = schwertmannite, Jt = jarosite, (t) = trace
‡ Mole ratio

suspension that was held at 60°C for 12 min, then cooled and dialyzed for 30 days against distilled water using cellulose membranes with an average pore radius permeability of 2.4 nm. The dialysis water was changed every other day. The final, washed precipitates of schwertmannite were transferred to 2-L polyethylene bottles and allowed to stand at 25°C in a constant-temperature room with occasional shaking. Starting pH values of the suspensions were 3.94, 3.91, and 3.93.

Two types of samples were periodically removed during the ensuing 1739 days. Immediately after shaking, an aliquot of the suspension was taken and centrifuged to concentrate the solid phase, which was then air-dried and analyzed for mineralogical composition by X-ray diffraction (XRD), for particle morphology by transmission electron microscopy (TEM) and for specific surface area by dinitrogen adsorption according to the method of Brunauer, Emmett, and Teller (BET) (Brunauer et al., 1938). A second aliquot was removed from the clear supernatant following gravity sedimentation of the suspended solid. This solution was filtered and analyzed for total Fe by the *o*-phenanthroline method (Sandell, 1944) and for SO_4 by ion chromatography; the latter analysis yielded no indication of a NO_3 contaminant. The solution pH was also measured in the clear supernatant. The total iron and SO_4 concentrations were converted to Fe^{3+} and SO_4^{2-} activities using the MINTEQ A2 computer program and the thermodynamic data contained therein (Allison et al., 1991). All relevant Fe(III)-, OH-, and SO_4-containing solution species were considered in the calculations.

2.2. Field Studies (Coal Mine Drainage)

Mine waters and associated ochre deposits were collected at periods of low or base stream flow from twenty-eight sites in the Ohio coalfield during September and October of 1987. The sampling strategy involved two major objectives. First, it was considered important to obtain water and sediment samples representing a wide range of geochemical conditions, especially in terms of drainage pH. Secondly, situations where effluents and associated precipitates could be directly related to each other and to point sources of discharge were emphasized whenever possible. The locations of all sample sites are given in Winland et al. (1991).

2.2.1. Water samples

Water temperature and pH were measured in the field, and quadruplicate solution samples were collected in acid-washed, Nalgene bottles after rinsing thoroughly with the local stream water. Solutions were not filtered in the field, but care was taken to exclude sediments and to minimize atmospheric contact. All samples were then transported to the laboratory on ice. After warming to room temperature, laboratory pH and electrical conductivity (EC) were measured on two of the four solution samples. The remaining duplicates were filtered through 0.2-μm Nucleopore membranes. Each filtrate was then split into two subsamples, one of which was acidified to pH < 2 with double distilled HNO_3 for measurement of dissolved metals,

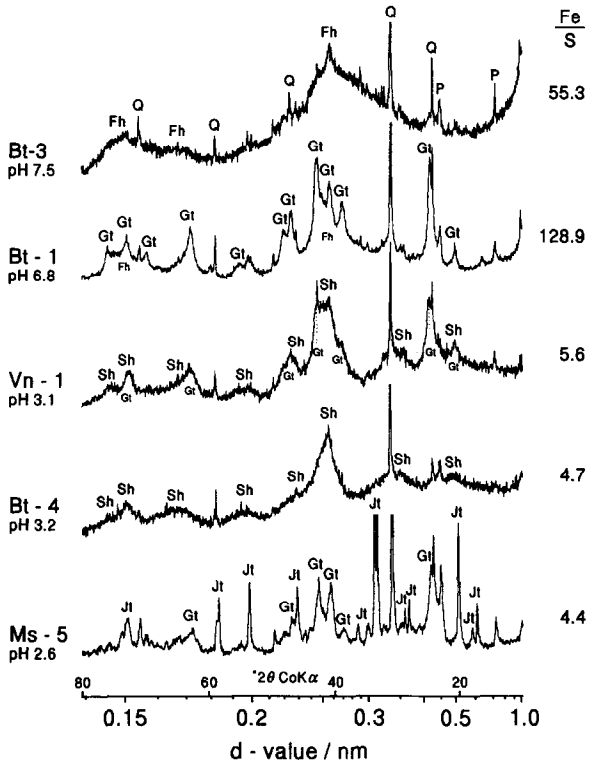

FIG. 1. Representative X-ray patterns from the mine drainage precipitates described in Table 1. Sample Bt-3 is composed primarily of ferrihydrite (Fh); sample Bt-1 of goethite (Gt) + Fh; sample Bt-4 of schwertmannite (Sh); sample Vn-1 of Gt + Sh; and sample Ms-5 of Gt + jarosite (Jt). Quartz (Q) and phyllosilicates (P) occur as detrital phases.

including Fe. The remaining subsample was not acidified and was used for analysis of SO_4, Cl, and Fe(II). The latter was determined within 24 h of collection.

Total concentrations of Al, Mn, Ca, Mg, and Fe were measured with atomic absorption spectrometry. Sodium and K were analyzed with the same instrument in flame emission mode. Dissolved Si was determined by the molybdate blue method of Skougstad et al. (1979), P by the molybdate blue method of the American Public Health Association (1985), and Fe(II) by the 2,2-bypyridine technique (Skougstad et al., 1979). Dissolved SO_4 and Cl were measured simultaneously by ion chromatography. Trace metal concentrations (B, Ba, Co, Cu, Cd, Cr, Ni, and Zn) were also determined but are reported elsewhere (Winland et al., 1991).

Geochemical modeling of aqueous-phase chemical equilibria was conducted with the MINTEQ A computer program (Felmy et al., 1983). Field water temperatures and pH values were used as model inputs along with laboratory measurements of dissolved Al, Fe(II), Fe, Mn, Ca, Mg, Na, K, Si, B, Ba, Cu, Cd, Cr, Ni, Zn, SO_4, and Cl. Ionic strength corrections were made using the Davies equation. Carbonate and HCO_3^- activities were estimated by assuming the systems to be at equilibrium with atmospheric CO_2.

2.2.2. *Sediment samples*

Approximately 40 L of suspension enriched with ochreous precipitate were collected in plastic containers at each site. Loose sediments were removed from the stream bottom using a hand-operated pump fitted with a plastic screen to minimize contamination from detrital mineral fragments. The precipitates were then concentrated in the laboratory by gravity sedimentation and centrifugation, washed by dialysis as described previously, quick-frozen, and freeze-dried. Total chemical analyses of the precipitates for both major and minor elements were conducted and are reported by Winland et al. (1991). In addition, oxalate-extractable Fe (Fe_o) was measured according to the method of Schwertmann (1964) using a 15 min extraction time, and the mineralogical composition of the precipitates was evalutated by XRD analysis of powdered specimens as described by Bigham et al. (1990).

2.3. Field Studies (Naturally Acid Stream)

A naturally acid alpine stream in the Zillertaler Alps, Austria, was identified and sampled using procedures similar to those described above (Schwertmann et al., 1995). Both water and sediment samples were collected from the stream course at several locations between the source (a spring draining a pyritic schist at ca. 2600 m asl) and the valley floor (ca. 2000 m asl). Ochreous bottom sediments were concentrated by sieving and gravity sedimentation, air-dried, and analyzed by XRD. Water samples were analyzed for pH, Eh, temperature, and dissolved K, Fe(II), Fe, and SO_4. The nonequilibrium, reaction path program, EQ6, was used to describe mineral precipitation processes occurring within the stream environment (Wolery et al., 1990; Wolery and Daveler, 1992). EQ6 computes reaction path models for both kinetic and stepwise equilibrium processes. These models can be applied to closed and simple open systems. The current simulation involved reaction of the acid, alpine spring water with dolomite [$(Ca, Mg)CO_3$] resulting in an increase in solution pH comparable to that observed in the field.

3. RESULTS AND DISCUSSION

3.1. Mineralogy of Natural Precipitates

The mineralogy of the natural precipitates collected from mine drainage in Ohio varies with the pH of the source waters (Table 1, Fig. 1). Those precipitates formed at pH 6.5 or higher are composed of 2-to-4-XRD-line ferrihydrite (nominally $Fe_5HO_8 \cdot 4H_2O$) or a mixture of ferrihydrite and goethite (α-FeOOH), whereas those precipitated from waters having pHs in the range of 2.8 to 4.5 are predominantly schwertmannite with trace to minor amounts of associated goethite and/or jarosite. Waters of intermediate pH (4.5 to 6.5) produced mixtures of ferrihydrite and schwertmannite. Only one sample, that formed at pH 2.6, contained a significant amount of jarosite [$(H, K, Na)Fe_3(OH)_6(SO_4)_2$].

Both schwertmannite and ferrihydrite dissolve completely in a pH 3.0 solution of ammonium oxalate, whereas goethite and jarosite do not. Consequently, as the content of goethite and/or jarosite in a precipitate increases, the ratio of oxalate-soluble to total oxide Fe (Fe_o/Fe_{tot}) decreases. This relationship is apparent in Table 1, with those samples containing significant amounts of goethite and jarosite yielding the lowest Fe_o/Fe_{tot} ratios.

The precipitates are also partitioned on the basis of their Fe_{tot}/S_{tot} molar ratios. Bigham et al. (1990) reported that the Fe_{tot}/S_{tot} mole ratio for schwertmannite typically ranges between 4.6 and 8. The schwertmannitic samples in this study yielded an average ratio of 5.4. Those samples with ratios lower than 5.4 usually also contained trace amounts of jarosite, which ideally has $Fe_{tot}/S_{tot} = 1.5$. The relatively high value of 4.4 obtained for the most jarositic specimen, Ms-5, is a result of dilution by goethite. Both goethite and ferrihydrite may adsorb SO_4, especially at low pH where their net surface charge is positive, but the total quantity of SO_4 associated with the solid phase is small compared to schwertmannite or jarosite. Full coverage of a goethite

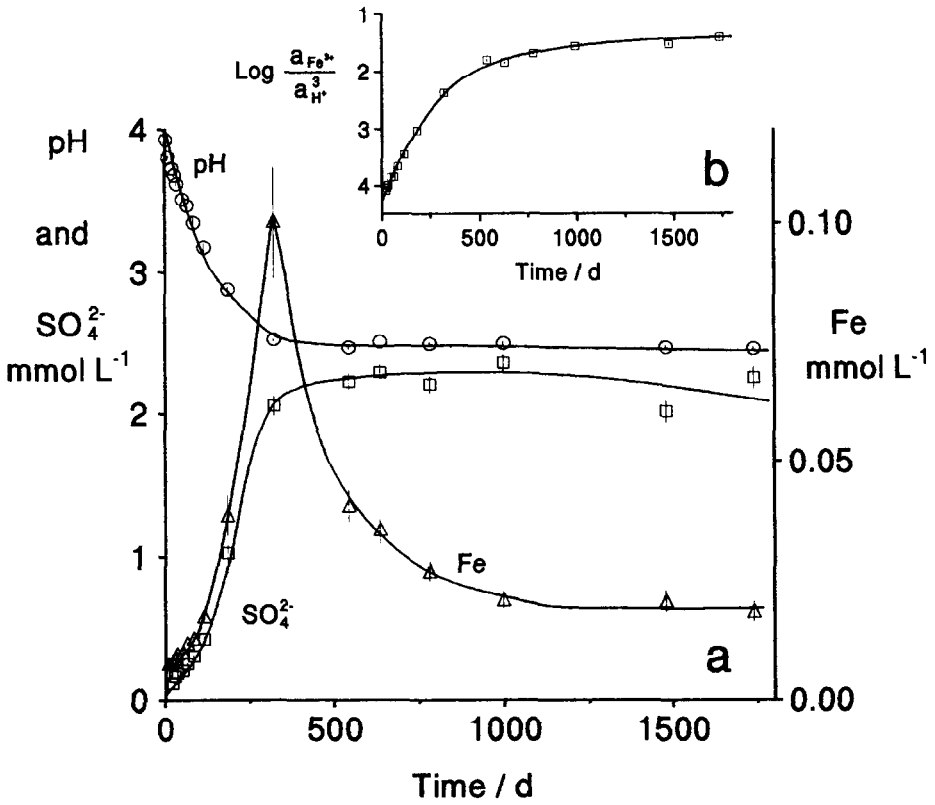

FIG. 2. (a) Changes in pH, SO_4, and iron with time for a beginning suspension of synthetic schwertmannite in water. Inset (b) shows a plot of log K_{Gt} = log $[a_{Fe^{3+}}/(a_{H^+})^3]$ as a function of time. The final, equilibrium value from three replicates was log K_{Gt} = 1.40 ± 0.01.

surface (80 m^2/g) with adsorbed sulfate would correspond to 2.5 μmol SO_4/m^2 and would yield an Fe_{tot}/S_{tot} ratio of 50. Accordingly, ratios for the ferrihydritic and goethitic samples in this study range from 37 (Tu-4) to 480 (Jf-1). These results show that it is possible to use relatively simple chemical analyses to arrive at a gross mineralogical composition for precipitates from ASW. On the other hand, positive identification of these poorly crystalline mineral phases can normally be achieved using standard powder XRD techniques and should be attempted whenever possible (Fig. 1).

3.2. Schwertmannite Stability and Goethite Solubility

The occurrence of goethite in at least trace amounts across the full range of mine drainage precipitates, including most of those dominated by schwertmannite (Table 1), suggests that goethite is ultimately the most stable mineral phase associated with ASW. To test this possibility, a synthetic specimen of schwertmannite was placed in contact with distilled water and changes in both solution chemistry and solid phase mineralogy were monitored over time. The specimen of schwertmannite used in this study had the composition $Fe_8O_8(OH)_{5.5}(SO_4)_{1.25}$ (the same as sample B-2000S in Bigham et al., 1990). Figure 2 shows the changes in solution pH, Fe, and SO_4 concentrations over a period of 1739 days.

During this time, the pH dropped from 3.9 to 2.4 whereas the concentration of SO_4 increased to a level of 2.2 mmol L^{-1}. Schwertmannite also proved to be unstable relative to goethite under these experimental conditions. Traces of goethite were detected by XRD as early as 65 days after beginning the study, and by 543 days the transformation was essentially complete (Fig. 3). The observed changes in solution pH and SO_4 reflect the gradual hydrolysis of schwertmannite while converting to goethite via the overall reaction:

$$Fe_8O_8(OH)_{5.5}(SO_4)_{1.25(s)} + 2.5\ H_2O_{(l)} \Rightarrow 8\ FeOOH_{(s)} + 2.5\ H^+_{(aq)} + 1.25\ SO^{2-}_{4(aq)}. \quad (1)$$

The apparent nonstoichiometric release of Fe and SO_4 (Fig. 2) in the early stages of mineral dissolution reflects the fact that a significant fraction of the SO_4 associated with the formula of schwertmannite is specifically adsorbed to the mineral surface (Bigham et al., 1990). This surface-sorbed SO_4 cannot be discounted because it appears to have a stabilizing influence on the high surface area mineral particles. Thus, a complete description of aqueous solubility relationships for schwertmannite would presumably require a combination of solubility calculations and surface complexation modeling that is beyond our current capabilities.

Total dissolved iron showed a well-defined peak at around 320 days before stabilizing at about 0.02 mmol L^{-1} after 1000 d. This "spike" of dissolved iron could arise from the fact that continuous mixing was not carried out in this

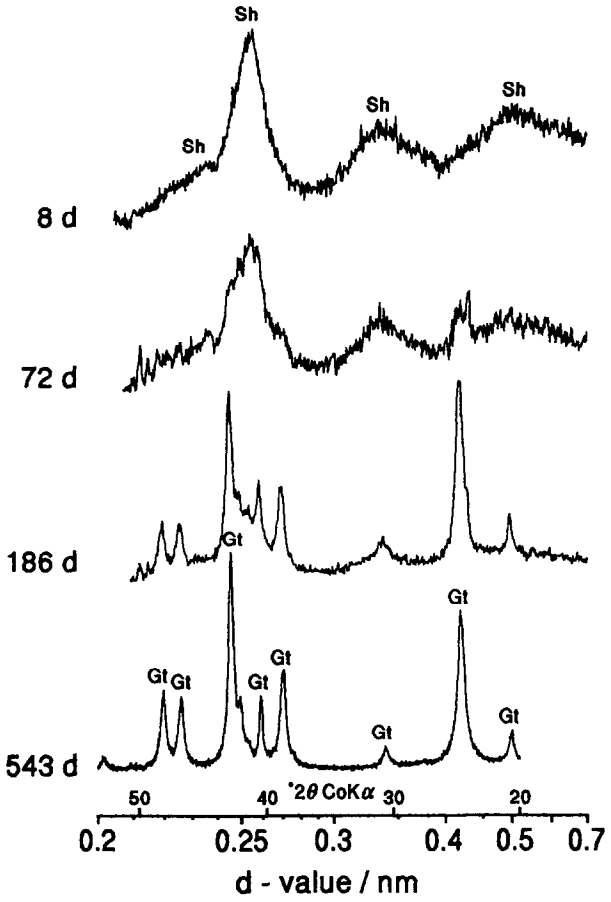

FIG. 3. X-ray diffractograms showing the transformation of synthetic schwertmannite to goethite over 543 days.

experiment. Because the rate of nucleation and crystal growth usually increases with increasing degree of supersaturation, it may also mark the point where the rate of goethite formation became greater than the rate of schwertmannite dissolution. A plot of log $(a_{Fe^{3+}}/(a_{H^+})^3)$ as a function of time (Fig. 2b) with speciation data from the MINTEQ A2 program yields a plateau from which a log K_{Gt} of 1.40 ± 0.01 was calculated in accordance with the reaction:

$$FeOOH_{(s)} + 3\ H^+_{(aq)} \Leftrightarrow Fe^{3+}_{(aq)} + 2\ H_2O_{(l)}. \quad (2)$$

This solubility product for goethite is substantially higher than the value of log $K_{Gt} = -1.0$ recommended by Nordstrom et al. (1990) or the value of −0.02 given by Lindsay (1979). Differences between both the reference data and the result obtained in the current experiment may be due, in part, to the lack of an internally consistent set of data from which to perform the necessary solubility calculations.

Another possibility is that the current experimental results reflect a strong particle-size effect on goethite solubility. The log K_{so} of small (<1 μm) crystals increases with decreasing particle size. According to Tardy and Nahon (1985)

$$\log K_{so} = \log K_{so}(\text{bulk}) + 27/d, \quad (3)$$

where "d" is the diameter of a spherical particle in nm. Electron micrographs of the starting schwertmannite and final goethite are shown in Fig. 4. From these data the average length and width of sixty goethite particles were determined to be 140 and 35 nm, respectively. Moreover, using the Scherrer formula, mean crystallite lengths in the a (MCL_a) and b (MCL_b) dimensions were calculated from the corrected integral widths at half height of the 021, 040, and 060 and the 110, 130, 101, 111, and 140 XRD peaks, respectively (MCL_c cannot be calculated from the XRD patterns). The resulting values were 15 nm for MCL_a and 24 nm for MCL_b. The thickness of the particles, i.e., the smallest dimension of the parallelepiped is given by MCL_a, while the width is MCL_b (30 nm from an average of TEM and XRD measurements), and the length is MCL_c (140 nm). A sphere of equal

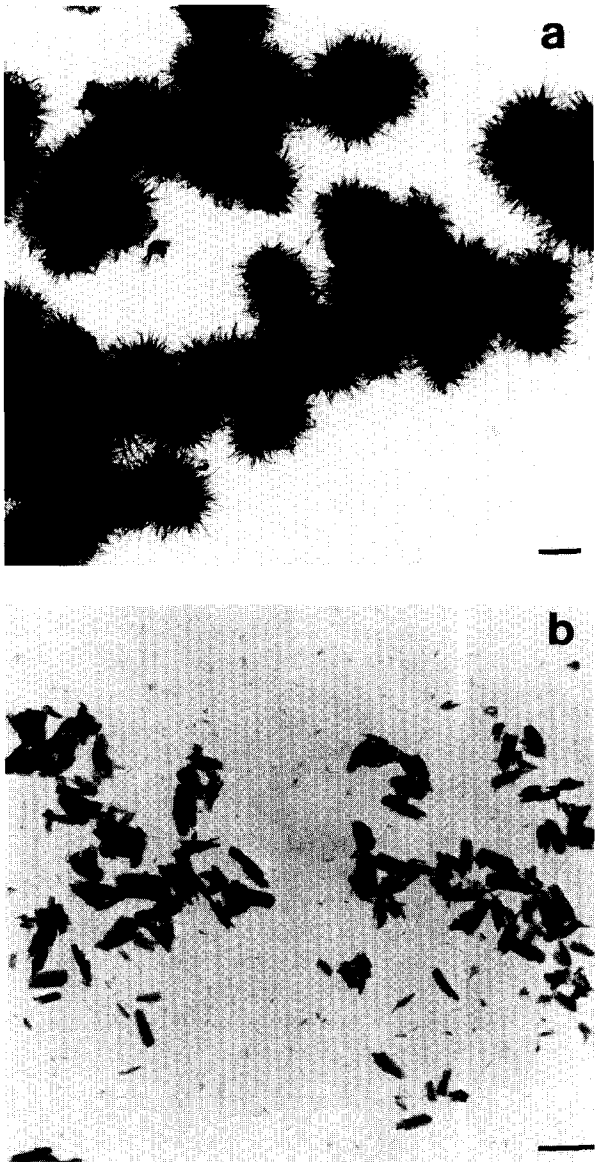

FIG. 4. Transmission electron micrographs of the starting schwertmannite (a) and the final goethite (b) in the stability experiment. Scale bar = 200 nm.

Table 2. Temperature and chemistry of Ohio mine drainage waters

Site	Temp. K	EC μScm^{-1}	pH	Fe(II)	Fe	Al	Mn	Si	Ca	Mg	Na	K	SO4	Cl
				μmol L^{-1}				mmol L^{-1}						
Bt-1	292	166	6.8	nd†	70	19	16	0.13	4.40	2.62	13.92	0.16	12.80	0.78
Bt-3	291	185	7.5	nd	7	26	25	0.12	6.36	3.18	10.09	0.19	11.53	0.97
Bt-4	291	162	3.2	1970	2276	1572	58	0.64	4.17	1.30	2.14	0.05	13.09	0.80
Cs-1	287	117	3.3	224	516	152	144	0.46	2.92	1.57	1.74	0.17	6.48	1.55
Ho-1	286	94	4.2	326	394	341	132	0.52	2.32	2.14	1.09	0.16	5.66	0.68
Jf-1	288	103	7.3	5	7	4	8	0.17	2.62	1.48	6.13	0.18	2.24	0.63
Jf-2	290	322	7.8	nd	2	7	21	0.33	7.25	3.59	24.88	0.29	21.13	1.35
Jf-3	288	145	3.8	9	34	408	300	0.63	6.66	3.09	1.15	0.12	10.66	0.74
Jk-1	288	182	5.9	621	720	345	370	0.38	7.19	2.68	4.24	0.28	13.24	0.50
Jk-2	289	37	4.9	127	195	41	29	0.38	1.21	0.2	0.23	0.06	1.85	0.22
La-1	279	150	3.1	1232	1676	1557	45	0.91	5.48	1.39	1.20	0.12	12.93	1.23
Me-1	286	139	3.7	358	466	178	156	0.61	4.16	2.35	4.30	0.17	9.38	0.78
Ms-1	286	170	5.8	2292	2471	11	74	0.34	3.59	1.70	5.87	0.25	15.53	0.68
Ms-2	288	106	6.1	922	931	4	62	0.25	2.57	1.20	3.36	0.17	7.92	2.17
Ms-3	298	210	2.8	1445	2229	534	378	0.79	5.46	2.90	1.85	0.23	17.38	0.37
Ms-5	300	375	2.6	2811	5748	815	432	0.79	6.58	6.25	8.13	0.30	36.40	0.32
Nb-1	287	404	3	347	1443	3521	2435	0.93	14.36	19.79	0.47	0.29	45.21	1.11
Pr-1	298	417	3.2	6177	8630	241	2818	0.58	10.21	14.64	1.06	0.27	42.66	0.45
Pr-2	298	273	2.8	668	2399	1075	1456	0.68	6.04	7.20	2.84	0.22	24.89	1.39
Pr-3	288	151	3.3	134	421	89	165	0.43	3.14	1.78	4.65	0.22	8.36	1.62
Pr-4	287	171	3.8	528	641	237	78	0.55	2.71	1.73	7.00	0.17	8.08	0.70
Pr-5	---	160	3.1	1468	2471	3210	136	-----	1.90	1.08	1.05	2.13	10.62	-----
Tu-1	289	285	2.9	850	2113	1353	629	0.71	9.70	4.81	2.58	0.22	24.91	0.32
Tu-2	299	223	3.2	571	865	56	173	0.39	8.15	2.53	5.44	0.31	16.41	0.30
Tu-3	290	194	3.2	485	992	222	350	0.36	5.47	2.58	3.28	0.24	13.43	0.41
Tu-4	288	115	6.8	64	70	30	329	0.19	4.64	3.02	0.58	0.15	6.67	0.25
Vn-1	286	195	3.1	2202	3223	482	132	0.91	4.08	2.02	4.85	0.23	13.14	0.34
Wa-1	288	315	3.8	304	414	2380	1238	0.48	11.01	11.23	0.78	0.19	27.78	0.86

†nd = not detected

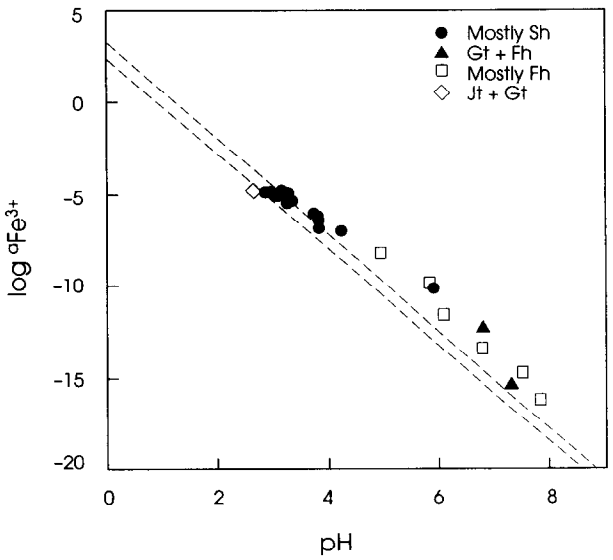

FIG. 5. Plot of Fe^{3+} activity against pH for Ohio mine drainage waters against a solubility window defined by log $a_{Fe^{3+}}$ = 3.03−2.60 pH and log $a_{Fe^{3+}}$ = 2.40−2.60 pH for schwertmannite [log IAP_{Sh} = 18.0 ± 2.5]. Window computed using an average log $a_{SO_4^{2-}}$ = −2.32.

volume would then be 49 nm in diameter and the adjusted log K_{Gt}, using a bulk log K_{Gt} of −0.02 (Lindsay, 1979) and Eqn. 3, would be 0.53. If only the smallest particles are considered (width = 34, breadth = 9, thickness = 3.6 nm), the same calculation would yield log K_{Gt} = 2.1.

Surface areas of the goethites were also measured using N_2 adsorption and the triple-point BET method. Results varied from 63 to 99 m^2/g and yielded values of log K_{Gt} ranging from 1.2 to 1.9 according to Eqn. 3 and the solubility data of Lindsay (1979). Our experimental value from the equilibrium study is, once again, consistent with the range suggested by these measurements. Deviations would obviously be greater in all cases if the value proposed by Nordstrom et al. (1990) is used as the bulk solubility product for goethite.

Solubilities higher than the "ideal" are probably typical of the poorly crystalline goethites associated with ASW. It is also apparent from Fig. 1 that the decay of schwertmannite can temporarily produce dissolved iron concentrations that are 0.5−1 order of magnitude higher than those represented by the proposed equilibrium situation for goethite. This observation may be relevant to the frequently reported supersaturation of ASW with respect to iron.

3.3. Schwertmannite Solubility

Aqueous equilibrium for a schwertmannite of composition $Fe_8O_8(OH)_x(SO_4)_y$, where $8 - x = 2y$ and $1.0 \leq y \leq 1.75$, would ideally be described by the reaction:

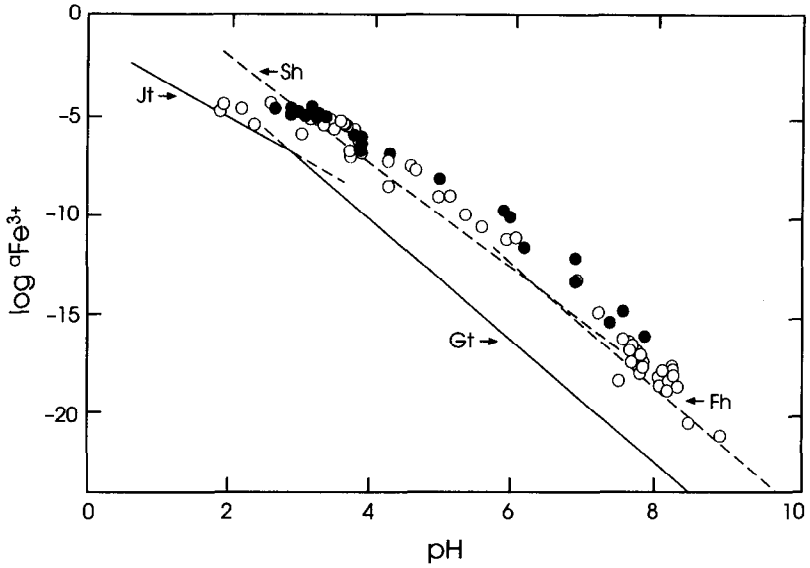

FIG. 6. Plot of Fe^{3+} activity against pH for combined data from Ohio (closed circles) and Leviathan mine drainage waters (open circles as presented in Nordstrom, 1991) with solubility lines for Gt = goethite (log $a_{Fe^{3+}}$ = 1.40–3 pH), Jt = K-jarosite (log $a_{Fe^{3+}}$ = −0.30–2 pH), Fh = ferrihydrite (log $a_{Fe^{3+}}$ = 5.0–3 pH), and Sh = schwertmannite (log $a_{Fe^{3+}}$ = 2.67–2.60 pH) added. Solubility lines calculated using an average log $a_{SO_4^{2-}}$ = −2.32, an average log a_{K^+} = −3.78, and log K_{so} values for Gt, Jt, Fh, and Sh of 1.40, −12.51, 5.0 and 18.0, respectively.

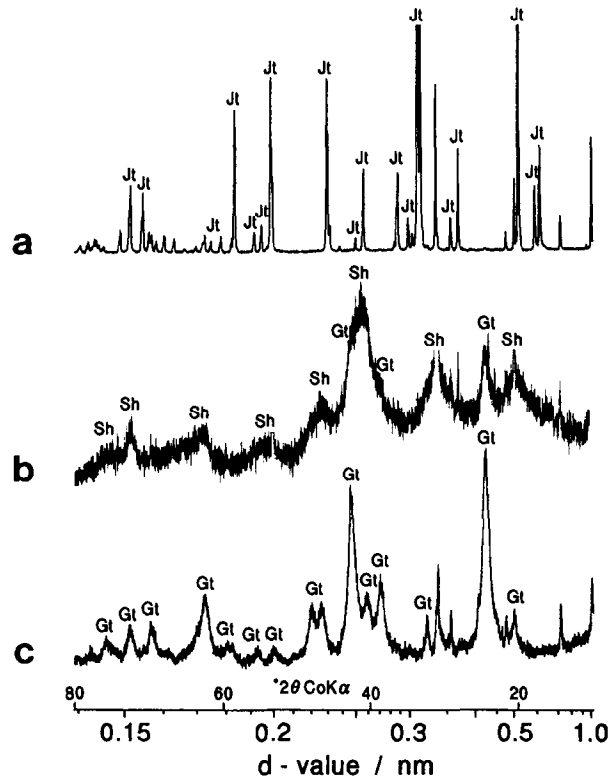

FIG. 7. X-ray diffraction patterns of precipitates from a naturally acid alpine stream showing (a) jarosite (Jt) at the source, (b) schwertmannite (Sh) formed at pH 3–5, and (c) goethite (Gt) formed at pH > 7.

$$Fe_8O_8(OH)_x(SO_4)_{y(s)} + (24 - 2y)\,H^+_{(aq)} \Leftrightarrow$$

$$8\,Fe^{3+}_{(aq)} + y\,SO^{2-}_{4(aq)} + (24 - 2y + x)/2\,H_2O_{(l)}. \quad (4)$$

The corresponding aqueous solubility product for this dissolution reaction would be given by

$$\log K_{Sh} =$$

$$8 \log a_{Fe^{3+}} + y \log aSO_4^{2-} + (24 - 2y)\,\text{pH}. \quad (5)$$

However, the calculation of a solubility product "constant" for schwertmannite is probably impractical because of (a) inherent compositional variability, (b) the occurrence of sulfate as both a structural and surface-sorbed species, and (c) the apparent instability of the mineral relative to goethite. A meaningful alternative might be to derive a solubility "window" such as that recognized for ferrihydrite (Nordstrom et al., 1990), a poorly crystalline mineral that is also metastable with respect to goethite in many surface environments (Schwertmann and Taylor, 1989).

Recent laboratory experiments involving the biological oxidation of Fe(II) at low pH suggest that the optimum pH for schwertmannite precipitation from ASW is in the range of 2.8 to 3.2 (Bigham et al., 1996). Several relatively pure specimens of schwertmannite were obtained from Ohio mine waters within this pH range (samples Bt-4, La-1, Ms-3, Nb-1, Pr-2, Tu-2, and Tu-3) (Table 1). To arrive at a solubility window for schwertmannite, the corresponding mine solution data (Table 2) were speciated using the MINTEQ A program (means for the solution parameters of interest were pH = 3.0 ± 0.2, log $a_{Fe^{3+}}$ = −5.05 ± 0.24, log $a_{SO_4^{2-}}$ = −2.22 ± 0.12), and compositions for the schwertmannites of interest were derived from the data presented in Table 1 (mean composition was $Fe_8O_8(OH)_{4.8}(SO_4)_{1.6}$). Similar

Table 3. Water chemistry from a naturally acid alpine stream

Sample	Temp. K	pH	Eh mV	Fe	Fe(II)	SO_4	K	Ppt.†
				µmol L^{-1}				
Spring								
Surface water	277	2.71	753	------	-----	3279	10	None
Pore water	278	2.78	792	423	25	27649	33	Jt
Stream Cross-Section‡								
15 cm	284	2.83	754	------	------	------	------	None
60 cm	284	2.83	755	------	------	------	------	None
90 cm	284	2.81	755	424	30	2311	15	None
110 cm	286	2.81	755	424	38	2176	10	None
115 cm	286	2.95	756	428	25	1999	13	None
120 cm	287	3.05	740	177	18	916	13	Sh, Gt
122 cm	------	3.48	-----	88	11	552	10	Sh, Gt
123 cm	------	3.76	-----	41	13	500	15	Sh, Gt
125 cm	287	4.20	666	21	4	260	13	Sh, Gt
130 cm	287	4.20	600	4	nd§	177	13	Sh, Gt

† Ppt. = precipitate; Jt = jarosite; Sh = schwertmannite; Gt = goethite.
‡ Cross section at confluence (left-to-right); see color plate.
§ nd = not detected

precipitates associated with solutions of higher pH were avoided because it was not possible to exclude post-precipitation dilution effects from extraneous surface waters. These seven sample sets were then used to calculate ion activity products (IAP) according to Eqn. 5. The results suggest that an appropriate solubility window for schwertmannite is defined by log $IAP_{Sh} = 18.0 \pm 2.5$.

3.4. Iron Activities and Water-Mineral Equilibria

Concentrations of major dissolved elements in the mine drainage waters collected in this study are summarized in Table 2. Speciation of these data with the MINTEQ A program showed, as expected, that the distribution of dissolved Fe(III) species was pH dependent. At pH < 3.5, the dominant Fe(III) species were the sulfate complexes, $FeSO_4^+$ and $Fe(SO_4)_2^-$, whereas at higher pH values the hydroxide complexes became prominent. The Fe^{3+} ion never exceeded more than 10% of the total reported Fe(III) concentration.

The output generated by MINTEQ A for log $a_{Fe^{3+}}$ in the Ohio mine waters is plotted relative to the proposed IAP window for schwertmannite in Fig. 5 using a mean value for log $aSO_4^{2-} = -2.38$ that was derived from the complete set of field samples. The window adequately describes most of the schwertmannitic samples associated with mine effluents in the pH range of 2.5 to 4.0. At higher pH values, the drainage waters are supersaturated with respect to the proposed window whereas the single water sample associated with jarosite is slightly undersaturated. A release of iron (and SO_4) upon dissolution of schwertmannite, as observed in the laboratory equilibrium study (Fig. 2), could lead to the apparent supersaturation with respect to Fe^{3+} at higher pH values. Alternatively, other solid phases may be controlling the activity of dissolved Fe^{3+} in these waters.

Figure 6 provides a comparison of the Fe^{3+} activity data generated by MINTEQ A for the Ohio mine waters with similar data from the Leviathan mine drainage system in California and Nevada (Nordstrom, 1991). The relationship between pH and log $a_{Fe^{3+}}$ is the same for both datasets and suggests that the results of this study can be extrapolated to other environments. Previously, Ball and Nordstrom (1989) had concluded that the Leviathan data reflected a control on Fe^{3+} activities by precipitation of ferrihydrite. Nordstrom (1991) subsequently noted that the log ($a_{Fe^{3+}}/a_{OH^-}$) slope was less than 3 over the pH range 3.5 to 7, in general agreement with the findings of Fox (1988), who reported a slope of 2.35 in a study of colloidal and dissolved Fe^{3+} in river waters. Nordstrom (1991) also suggested that the observed slope, which is equal to the OH/Fe ratio in the precipitate, could mean that SO_4 is a component of the suspended mineral phase as would be the case if schwertmannite is influencing the aqueous solubility of Fe^{3+} over this pH range.

The log $a_{Fe^{3+}}$ data in Fig. 6 actually appear to define three slopes. On the basis of our mineralogical work, those data in the pH range of 1.5 to 2.5 are probably influenced by the formation of jarosite, those above pH 5.5 by ferrihydrite, and those at intermediate pH values by schwertmannite. Assuming a log K_{Gt} of 1.40, all three minerals are metastable with respect to goethite above pH ~ 2; i.e., over much of the pH range associated with mine drainage waters. Placing the data in a proper geochemical perspective is also complicated by a variety of other factors, not the least of which is a widely variable reference base for the solubilities of jarosite and ferrihydrite. As noted previously for goethite, the only valid means of comparing such information is to access original solubility data and perform equilibrium calculations us-

FIG. 8. Color plate showing the confluence of a naturally acid alpine stream (left) with a non-acid tributary (right). Total width of stream at confluence is approximately 1.7 m; cross-section distances reported in Table 3 proceed from left to right. The ochreous precipitate is mostly schwertmannite. Location is near Pfitscher Joch in the Zillertaler Alps, Austria (see Schwertmann et al., 1995 for details).

ing the same speciation model. Given the difficulty of obtaining such data and documenting original experimental conditions, one can only assume that the true solubility products fall somewhere within the range of reported values.

Reported solubility products for K-jarosite range between −9.21 (Kashkay et al., 1975; Chapman et al., 1983) and −12.51 (Lindsay, 1979). Recent studies by Alpers et al. (1989) on seven jarosites from natural mine drainage waters showed 10 to 32 mole percent substitution of H_3O^+ and 3 to 15 mole percent substitution of Na^+ for K^+, but the average log K_{so} for these jarosite solid solutions was in general agreement (−9.34 vs. −9.21) with that given by Chapman et al. (1983) for K-jarosite. By contrast, the low pH data in Fig. 6 appear to be best described using a solubility line calculated using log K_{Jt} = −12.51.

The literature yields log K_{so} values for ferrihydrite ranging from 3 to 5 (Nordstrom et al., 1990), and the solubility of this phase undoubtedly varies with age of the precipitate as shown by Lengweiler et al. (1961). The data in Fig. 6 are at or near saturation with respect to ferrihydrite above pH 7 using log K_{Fh} = 5.0; lower solubility products would increase the degree of supersaturation. As noted previously, the activities of dissolved Fe^{3+} are adequately described in the pH range of 2.5 to 4.0 using the conditional IAP generated in this study for schwertmannite. ASW with pH values in the range of 4.0 to 7.0 are generally supersaturated with respect to both schwertmannite and ferrihydrite. This apparent supersaturation may reflect dissolution-reprecipitation effects similar to those shown in Fig. 2.

3.5. A Revised Model for Mineral Speciation

Thermodynamic equilibrium is probably rarely achieved in ASW because of spatial, temporal, and kinetic effects that continually perturb the local environment. A good example is provided by a recently identified alpine stream that is inherently acid and that has produced a natural occurrence of schwertmannite (Schwertmann et al., 1995). This stream originates as a spring in talus from a pyritic schist. The spring water (pH 2.3–2.8) is visibly clear but passes through sediment laden with jarosite (Fig. 7a). Approximately 100 m downslope, the clear spring water merges with a small, non-acid tributary producing a strong geochemical gradient across the watercourse (Table 3). Precipitation of schwert-

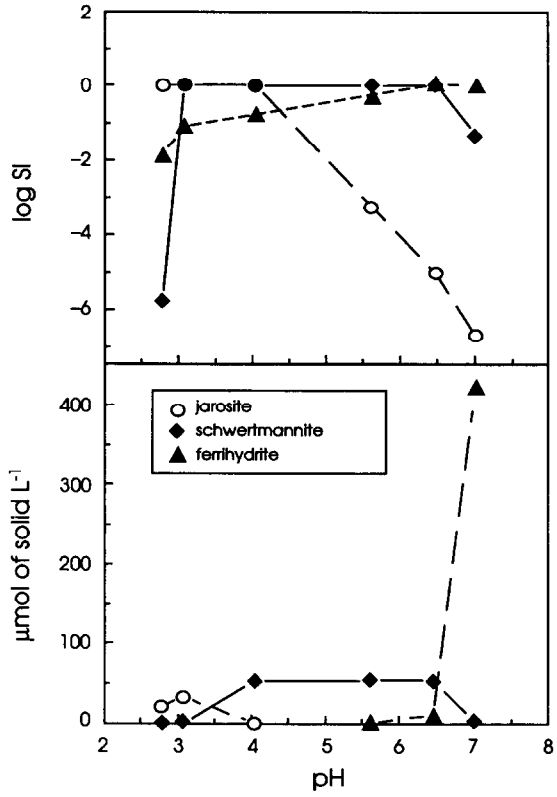

FIG. 9. Reaction path predictions of (a) saturation indices (SI) and (b) the concentrations of solid phases produced or consumed during reaction of 1 L of water from a naturally acid alpine stream with a calcareous (dolomitic) stream bed. Model calculations were made with the EQ 6 computer program and did not account for downstream dilution. Goethite was not permitted to form.

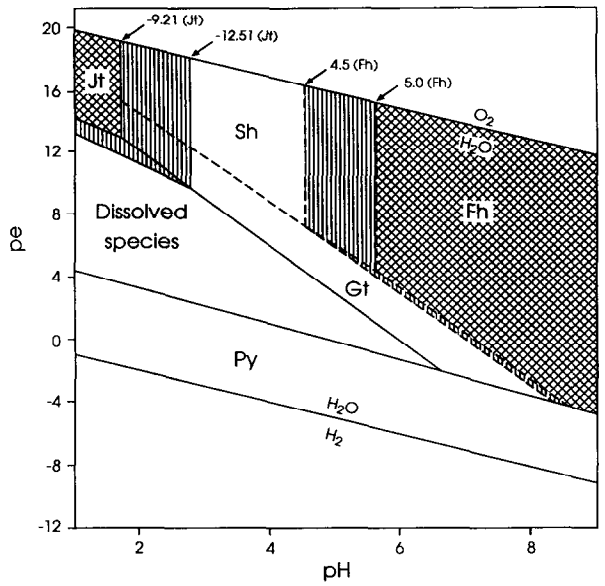

FIG. 10. pe-pH diagram for Fe–S–K–O–H system at 25°C where pe = Eh(mv)/59.2; total log activities of Fe^{2+} = −3.47; Fe^{3+} = −3.36 or −2.27); SO_4^{2-} = −2.32, K^+ = −3.78; log K_{so} values for solid phases as given in Fig. 6. Jt = K-jarosite, Sh = schwertmannite, Fh = ferrihydrite, Gt = goethite, Py = pyrite. Line equations are: Gt (pe = 17.9−3 pH); Jt (pe = 16.21−2 pH); Fh (pe = 21.50−3 pH), Sh (pe = 19.22−2.6 pH), and Py (pe = 5.39−1.14 pH). Fields of metastability shown by dashed lines. Single-hatched areas demonstrate expansion of K-jarosite and ferrihydrite fields if lower log K_{so}'s are selected.

mannite together with some goethite occurs where the pH reaches 3.0 (Fig. 7b), and the stream bed immediately becomes ochreous in appearance (Fig. 8). Further dilution occurs repeatedly downslope as the stream is joined by additional, non-acid tributaries. Eventually, the pH of the primary stream exceeds 7.0, and goethite becomes the dominant mineral phase deposited from solution (Fig. 7c). The presence of ferrihydrite is also indicated by Fe_o/Fe_{tot} ratios exceeding 0.6 (data not given).

The observed paragenetic relationship between jarosite, schwertmannite, and ferrihydrite can be simulated by permitting the "porewater" at the source of the acid spring (Table 3) to react with dolomite (the primary carbonate mineral in this region) using the nonequilibrium, reaction path model EQ6 (Wolery et al., 1990) and the solubility data derived from this study. When goethite is prohibited from forming, the model calculations describe a series of dissolution and precipitation events downstream from the source. At pH 2.78, EQ6 indicates equilibrium of the porewaters with jarosite, and undersaturation with respect to schwertmannite and ferrihydrite (Fig. 9). At a solution pH value of approximately 3, saturation with respect to schwertmannite occurs. Above pH 4, jarosite is fully dissolved and schwertmannite becomes the dominant Fe phase. Above pH 6, saturation with ferrihydrite is achieved at the expense of schwertmannite.

Results such as these suggest that a model describing mineral-solution equilibria in ASW on the basis of strict equilibrium thermodynamics is unrealistic. Nevertheless, models that give proper consideration to both theory and the realities of nature will continue to provide an important means of interpreting the chemistry of ASW. In this spirit, we suggest that Fig. 10 represents an improved description of mineral-solution relationships in sulfate-rich waters.

Figure 10 is a pE-pH diagram for the Fe–S–K–O–H system calculated using the mineral solubility values reported previously and the average aqueous activities of relevant chemical species in the mine waters described in this study. Similar chemical activities for natural waters have been reported in other investigations (e.g., Brown, 1971; Van Breemen and Harmsen, 1975). According to Fig. 10, jarosite and goethite are the phases that ultimately control the solubility of iron in mine drainage waters. The jarosite stability field would be enhanced by higher SO_4^{2-}/K^+ activities and/or the selection of a lower log K_{Jt}, such as the value of −12.51 proposed by Lindsay (1979) (Fig. 10). Under the conditions defined for this diagram, schwertmannite is unstable with respect to goethite over the pH range 2 to 6. At higher pH values, ferrihydrite is formed but is also unstable with respect to goethite. The field of metastability for schwertmannite is markedly influenced by a change in log K_{so} of either jarosite or ferrihydrite (Fig. 10).

A field example of the gradual transformation of ferrihydrite to goethite has previously been reported (Bigham et al., 1992), and the instability of schwertmannite relative to goethite was demonstrated in this study. Higher dissolved iron and sulfate concentrations in natural ASW may tend to preserve schwertmannite in the field; however, other laboratory studies in which synthetic schwertmannite was equilibrated against a solution containing 2000 mg/L SO_4 (as Na_2SO_4) also yielded transformation to goethite. Factors influencing the stability and aqueous solubility of schwertmannite clearly warrant further study.

Acknowledgments—The authors gratefully acknowledge the analytical support of Ms. G. Pfab. Field and laboratory assistance were also provided by Dr. H. Stanjek, Mr. H. Fechter, and Mr. C. Sperl. Dr. H.-Ch. Bartscherer provided the TEM photos, and Mrs. E. Schuhbauer carefully prepared the figures. This study was partially funded by the Deutsche Forschungsgemeinschaft under grant Schw 90/42-1. Direct financial assistance was provided to JMB by the Alexander von Humboldt Stiftung and the Deutscher Akademischer Austauschdienst. Additional salary and research support were provided by state and federal funds appropriated to the Ohio Agricultural Research and Development Center, The Ohio State University, Journal article no. 33-95.

Editorial handling: E. J. Reardon

REFERENCES

Allison J. D., Brown D. S., and Novo-Gradac K. J. (1991) MINTEQA2/PRODEF2, a geochemical assessment model for environmental systems: Version 3.0 user's manual. *United States Environmental Protection Agency Report No. EPA/600/3-91/021.* U.S. Govt. Printing Office.

Alpers C. N., Nordstrom D. K., and Ball J. W. (1989) Solubility of jarosite solid solutions precipitated from acid mine waters, Iron Mountain, California, U.S.A. *Sci. Géol. Bull.* **42,** 281–298.

American Public Health Association (APHA) (1985) *Standard Methods for the Examination of Water and Wastewater. 16th. ed.* U.S. Govt. Printing Office.

Ball J. W. and Nordstrom D. K. (1989) Final revised analyses of major and trace elements from acid mine waters in the Leviathan mine drainage basin, California and Nevada—October 1981 to

October 1982. *U.S. Geological Survey Water-Resources Investigations Report* **89-4138.**

Bigham J. M., Schwertmann U., Carlson L., and Murad E. (1990) A poorly crystallized oxyhydroxysulfate of iron formed by bacterial oxidation of Fe(II) in acid mine waters. *Geochim. Cosmochim. Acta* **54,** 2743–2758.

Bigham J. M., Schwertmann U., and Carlson L. (1992) Mineralogy of precipitates formed by the biogeochemical oxidation of Fe(II) in mine drainage. In *Biomineralization Processes of Iron and Manganese: Modern and Ancient Environments* (ed. H. C. W. Skinner and R. W. Fitzpatrick), *Catena Suppl. 21,* pp. 219–232. Catena Verlag.

Bigham J. M., Carlson L., and Murad E. (1994) Schwertmannite, a new iron oxyhydroxysulfate from Pyhäsalmi, Finland, and other localities. *Mineral. Mag.* **58,** 641–648.

Bigham J. M., Schwertmann U., and Pfab G. (1996) Influence of pH on mineral speciation in a bioreactor simulating acid mine drainage. *Appl. Geochim.* **11** (in press).

Brown J. B. (1971) Jarosite-goethite stabilities at 25°C, 1 ATM. *Mineral. Deposita* **6,** 245–252.

Brunauer S., Emmett P. H., and Teller E. (1938) Adsorption of gases in multimolecular layers. *J. Amer. Chem. Soc.* **60,** 309–319.

Chapman B. M., Jones D. R., and Jung R. F. (1983) Processes controlling metal ion attenuation in acid mine drainage streams. *Geochim. Cosmochim. Acta* **47,** 1957–1973.

Felmy A. R., Girvin D. C., and Jenne E. A. (1983) MINTEQ A computer program for calculating aqueous geochemical equilibria. Final Project Rep., USEPA contract 68-03-3098. USEPA, Arlington, VA.

Fox L. E. (1988) The solubility of colloidal ferric hydroxide and its relevance to iron concentrations in river water. *Geochim. Cosmochim. Acta* **52,** 771–777.

Jambor J. L. (1994) Mineralogy of sulfide-rich tailings and their oxidation products. In *The Environmental Geochemistry of Sulfide Mine Wastes* (ed. D. W. Blowes and J. L. Jambor); *M.A.C. Short Course Handbook* **22,** 59–102.

Kashkay C. M., Borovskaya Y. B., and Babazade M. A. (1975) Determination of $\Delta G^{\circ}_{f,298}$ of synthetic jarosite and its sulfate analogues. *Geochem. Interl.* **12,** 115–121.

Lindsay W. L. (1979) *Chemical Equilibria in Soils.* Wiley.

Lengweiler H., Buser W., and Feitknecht W. (1961) Die Ermittlung der Löslichkeit von Eisen(III)-hydroxiden mit ^{59}Fe I. Fällungs- und Auflösungsversuche. *Helv. Chim. Acta* **41,** 796–805.

McKnight D. M. and Bencala K. E. (1989) Reactive iron transport in an acidic mountain stream in Summit County, Colorado: A hydrologic perspective. *Geochim. Cosmochim. Acta* **53,** 2225–2234.

Murad E., Schwertmann U., Bigham J. M., and Carlson L. (1994) Mineralogical characteristics of poorly crystallized precipitates formed by oxidation of Fe^{2+} in acid sulfate waters. In *Environmental Geochemistry of Sulfide Oxidation* (ed. C. N. Alpers and D. W. Blowes); *A.C.S. Symposium Series* **550,** 190–200.

Nordstrom D. K. (1991) Chemical modeling of acid mine waters in the western United States. USGS Water Res. Invest. Rep. No. 91-4034, pp. 534–538. U.S. Geol. Surv.

Nordstrom D. K. et al. (1990) Revised chemical equilibrium data for major water-mineral reactions and their limitations. In *Chemical Modeling of Aqueous Systems II* (ed. D. C. Melchior and R. L. Bassett); *A.C.S. Symposium Series* **416,** 398–413.

Sandell E. B. (1944) *Colorimetric Determination of Trace Metals.* Interscience Publ.

Schwertmann U. (1964) Differenzierung der Eisenoxide des Bodens durch photochemische Extraktion mit saurer Ammoniumoxalat-Lösung. *Z. Pflanzenernähr. Bodenkd.* **105,** 194–202.

Schwertmann U. and Taylor R. M. (1989) Iron oxides. In *Minerals In Soil Environments,* 2nd ed., Chap. 8, pp. 379–438. Soil Sci. Soc. Amer.

Schwertmann U., Bigham J. M., and Murad E. (1995) The first occurrence of schwertmannite in a natural stream environment. *European J. Miner.* **7,** 547–552.

Skougstad M. W., Fishman M. J., Friedman L. C., Erdmann D. E., and Duncan S. S. (1979) Methods for determination of inorganic substances in water and fluvial sediments. U.S. Geol. Survey Techniques of Water-Resources Investigations A1. U.S. Govt. Printing Office.

Tardy Y. and Nahon D. (1985) Geochemistry of laterites. Stability of Al-goethite, Al-hematite and Fe^{3+}-kaolinite in bauxites and ferricretes. An approach to the mechanism of concretion formation. *Amer. J. Sci.* **285,** 865–903.

Theobald P. K., Lakin H. W., and Hawkins D. B. (1963) The precipitation of aluminum, iron, and manganese at the junction of Deer Creek with the Snake River in Summit County, Colorado. *Geochim. Cosmochim. Acta* **27,** 121–132.

Van Breemen N. and Harmsen K. (1975) Translocation of iron in acid sulfate soils: I. Soil morphology, and the chemistry and mineralogy of iron in a chronosequence of acid sulfate soils. *Soil Sci. Soc. Amer.* **39,** 1140–1148.

Winland R. L., Traina S. J., and Bigham J. M. (1991) Chemical composition of ochreous precipitates from Ohio coal mine drainage. *J. Environ. Qual.* **20,** 452–460.

Wolery T. J. and Daveler S. A. (1992) EQ6, a computer program for reaction path modeling of aqueous geochemical systems: theoretical manual, user's guide and related documentation. Version 7.0. Lawrence Livermore Laboratory, UCRL-MA-110662 PTN. 339 p.

Wolery T. J., Jackson K. J., Bourcier W. L., Bruton C. J., Viani B. E., Knauss K. G., and Delany J. M. (1990) Current status of the EQ3/6 software package for geochemical modeling. In *Chemical Modeling of Aqueous Systems II* (ed. D. C. Melchior and R. L. Bassett); *A.C.S. Symposium Series* **416,** 104–116.